

pected labeling sites are consistently higher than those expected not to be labeled. This result confirms that when ^{13}C -labeled III synthesized from $[1-^{13}\text{C}]$ acetate is converted into I, the latter is labeled in the same pattern as that directly derived from $[1-^{13}\text{C}]$ acetate.^{8,9}

Despite the considerable variation in the enrichment of various carbons as shown by relative intensities, which warrants further investigation, our data does clearly indicate that C-13 and -15 of I are enriched. A strong evidence thus is provided that III is the only carbon source for the biosynthesis of I, implying the bisfuran ring system is derived from the C_6 side chain of III. A mechanism for the C_6 to C_4 conversion has been proposed by Thomas,¹⁰ but experimental evidence is still not available. The typical alternating labeling pattern of III from $[1-^{13}\text{C}]$ acetate is indicative of the involvement of a single polyketomethylene unit rather than two preformed units in the biosynthesis of III, II, and I, although little has been reported of the pathway leading to III.

Acknowledgment. This study is supported by Public Health Service Grant ES00612 and Western Regional Research Project W-122.

References and Notes

- J. S. E. Holker and L. J. Mulheirn, *Chem. Commun.*, 1576 (1968).
- D. P. H. Hsieh, M. T. Lin, and R. C. Yao, *Biochem. Biophys. Res. Commun.*, **52**, 922 (1973).
- M. Biollaz, G. Büchi, and G. Milne, *J. Am. Chem. Soc.*, **92**, 1035 (1970).
- M. T. Lin and D. P. H. Hsieh, *J. Am. Chem. Soc.*, **95**, 1668 (1973).
- M. T. Lin, D. P. H. Hsieh, R. C. Yao, and J. A. Donkersloot, *Biochemistry*, **12**, 5167 (1973).
- For fermentation technique see D. P. H. Hsieh and R. I. Mateles, *Appl. Microbiol.*, **22**, 79 (1971).
- D. L. Fitzell, D. P. H. Hsieh, R. C. Yao, and G. N. La Mar, *J. Agric. Food Chem.*, **23**, 442 (1975).
- D. P. H. Hsieh, J. N. Seiber, C. A. Reece, D. L. Fitzell, S. L. Yang, J. I. Dalezios, G. N. La Mar, D. L. Budd, and E. Motell, *Tetrahedron*, **31**, 661 (1975).
- P. S. Steyn, R. Vleggaar, and P. L. Wessels, *J. Chem. Soc., Chem. Commun.*, 193 (1975).
- R. Thomas, personal communication to M. O. Moss, "Aflatoxin and Related Mycotoxins, Phytochemical Ecology", J. B. Harborne, Ed., Academic Press, London, 1972, p 140.

D. P. H. Hsieh, R. C. Yao, D. L. Fitzell, C. A. Reece

Department of Environmental Toxicology
University of California
Davis, California 95616

Received September 8, 1975

Solvated Nickel Atoms and Their Free Cluster Formation in Organic Media

Sir:

We recently reported that codeposition of metal vapors (atoms) with certain solvents allows the formation of very reactive high surface area metal slurries.^{1,2} Further work showed that significantly different clustered forms of each metal were observed when different solvents were employed.³ It seemed to be of importance to study these clustering processes in more detail for two reasons: (1) we have observed differing reactivity for these metal particles when formed in different solvents, and so anticipated the possibility of tailoring metal particles for specific purposes, and (2) to gain some understanding of the metal atom clustering processes in an organic matrix, which has not been studied previously even though there has been interest expressed in such studies.^{4,5} We report here some of our work with nickel.⁶

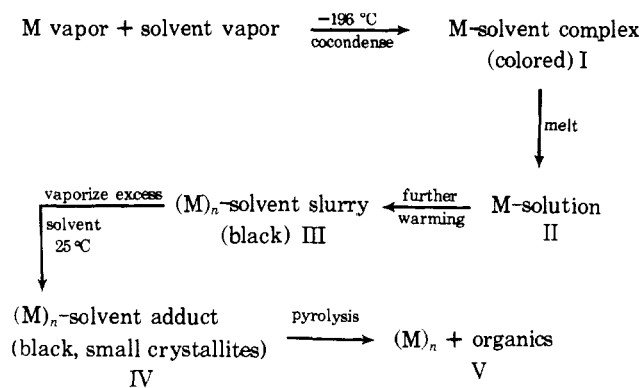
The clustering of nickel atoms in organic media is a process that has discrete stages (Scheme I). Stage I is a weak σ

Table I. Physical Data on Metal Particles (Stage IV)

M (solvent)	Solvent:metal ratio ^a	Surface area (m ² /g) ^b	Particle Size ^c (μ)
Ni(hexane)	1:25	45	5 × 20 rough pieces ^c
Ni(toluene)	1:40	100	0.5–0.8 spheres
Ni(THF)	1:3	400	0.5–1.5 spheres
Raney Ni ^d	- - -	80–100	90% 2–40

^a Determined by desorption of organics upon pyrolysis. ^b BET methods used except with Ni-THF where solvent and gas desorption was employed to calculate surface area. ^c Very rough edges and an average size (see SEM photos). ^d Grace #28. ^e Crystallite sizes could not be determined quantitatively due to the large line broadenings observed. These wide lines indicate crystallite sizes <100 Å, a region where the Scherrer equation does not apply. Relative crystallite sizes were determined by comparing the broad line coincident with the 111 reflection (d-spacing 2.01 Å) for commercial Ni powder utilizing Cu K α radiation: Raney Ni (2 θ broadening of 2°) > Ni-hexane (3° broadening) > Ni-toluene (4° broadening) > Ni-THF (8° broadening); commercial Ni powder (0.5° broadening). More detailed analysis of the Ni-toluene showed only the one broad line coincident with the 111 reflection, whereas Ni-THF showed two very broad lines, one corresponding to the 111 reflection and the other at lower angle with d spacing of about 4 Å.

Scheme I



or π complex formed when excess (>30:1) solvent is codeposited with the metal vapor. Stage II forms with some solvents upon low temperature melt down of the matrix. If well diluted, a homogeneous metal atom (or metal telomer) solution forms. On further warming small metal particles form, and the final size and shape of these particles is dependent on the solvent employed. Evaporation of excess solvent yields stage IV with little apparent sintering in going from III to IV. Examination of the stage IV particles has been carried out in some detail employing scanning electron microscopy, x-ray powder methods, and chemical methods. Description of three solvent systems follows (all solvents were freshly distilled from benzophenone ketal under purified nitrogen before use).

Ni-Hexane. A black matrix forms during codeposition due to metal cluster formation at $-196\text{ }^\circ\text{C}$. Upon melt down small particles form along with some larger flakes (that readily break up to smaller particles). These metal particles are pyrophoric and quite reactive with alkyl halides, even after removal of excess solvent under vacuum at room temperature (several hours pumping down to 5×10^{-3} Torr). Solvent retention ratio, surface area, particle size, and qualitative information on crystallite size are recorded in Table I. This Ni-hexane powder is an extremely active hydrogenation catalyst for both benzene and norbornene, more active than Raney Ni (Grace #28-W-2).

Ni-Toluene. A red-brown matrix forms during codeposition due to the formation of a toluene-Ni π -complex ($-196\text{ }^\circ\text{C}$).⁷ Deposition of triethyl phosphite on top of this matrix followed by melt down results in the formation of Ni-

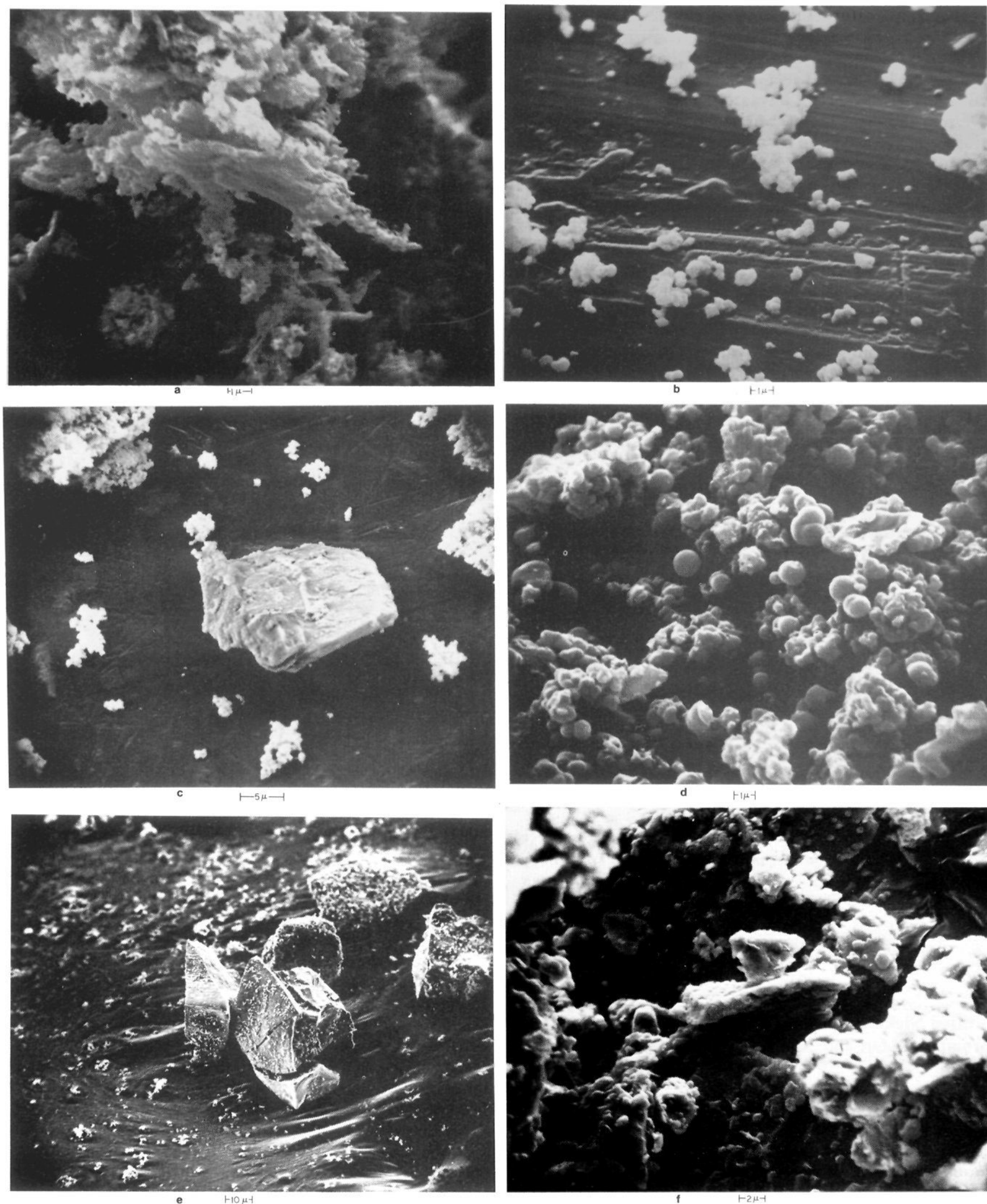


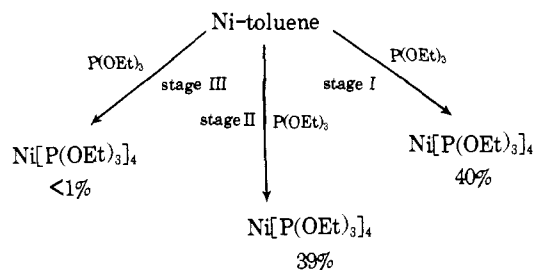
Figure 1. Scanning electron micrographs of Ni samples stages IV and V: (a) Ni-hexane, (b) Ni-toluene, (c) Ni-toluene after heating and sintering, (d) Ni-THF, (e) Ni-THF after heating and sintering, (f) Raney Ni.

$[P(OEt)_3]_4$ in 40% yield based on Ni evaporated. Other ligands behave similarly, readily displacing the weakly bound solvent, toluene. Melt down of the Ni-toluene matrix by itself results in the formation of a dark brown Ni-toluene solution. In several experiments (stage II Ni-toluene) this solution was allowed to melt down onto reactants such as triphenylphosphine, triethyl phosphite, allyl bromide, or benzyl chloride. Reactions took place as if metal atoms were

present. For example, if triethyl phosphite and the Ni-toluene solution were mixed a 39% yield of $Ni[P(OEt)_3]_4$ resulted. This nickel atom-nickel telomer toluene solution has been used for deposition of nickel on catalyst supports. The solution was allowed to flow down over solid supports such as Al_2O_3 , SiO_2 , molecular sieve, or activated carbon. On further warming of the solution small metal crystallites were deposited in the support. The deposition occurred at

fairly low temperature (about $-50\text{ }^{\circ}\text{C}$) in the reaction chamber. With Al_2O_3 the Ni was completely adsorbed (1–2% Ni loading) but did not change the overall surface area of the Al_2O_3 sample. On heating the Al_2O_3 -Ni powder in stages with a small flame, its surface area decreased after each heating until finally the area had fallen from 120 to 70 m^2/g . Apparently the small Ni crystallites sintered upon heating and blocked some of the pores in the Al_2O_3 sample.

When stage II Ni-toluene is allowed to warm to room temperature, stage III, a Ni-toluene slurry is formed. This clustered form of the Ni is not reactive with triethyl phosphite under the same conditions as stage I and II were, thus showing that solvated atoms are probably present both in stage I and II. Vacuum pumpoff of solvent leaves stage IV, pyrophoric, reactive Ni-toluene clusters (cf. Table I for properties).



Ni-THF. A yellow matrix forms upon codeposition that consists of a reactive, low temperature stable Ni(0)-etherate. This etherate is quite reactive with such things as alkyl halides causing reduction and coupling. Warming of the Ni-THF complex results in black streams of Ni-THF flowing to the bottom of the reactor. The resulting Ni-THF slurry is very finely divided and totally syringeable. It is also reactive with alkyl halides. After removal of THF under high vacuum pumping for several hours at room temperature, a very fine Ni-THF powder is formed that is a fairly unreactive hydrogenation catalyst, but a very good catalyst for cyclohexene disproportionation to benzene and cyclohexane. A great deal of residual THF is very strongly bound, which can only be displaced by strong ligands such as triethyl phosphite, but not by excess amines, alkenes, or ethers. The particles are surprisingly uniform as tiny spheres which upon strong heating release organics (THF (45%), butyraldehyde (20%), 1-butanol (30%), furan (5%)) with formation of larger Ni crystals, as shown by the SEM studies illustrated.

The process for producing these solvated metal atoms and clusters is very versatile since many metal-solvent combinations can be employed. Each stage (I-IV) in the clustering process can be useful in further chemical reactions.^{7,8} Furthermore, this method points toward wide extensions of Sinfelt's "bimetallic cluster" principle⁹ since two different metals could be clustered in the zero-valent state in a host of different matrices and then deposited on catalyst supports.

Acknowledgments. The generous support of the National Science Foundation (GP-42376) is greatly appreciated. We also are grateful for helpful discussions with Dr. Lewis Radonovich and the UND Medical School for the use of SEM equipment.

References and Notes

- (1) K. J. Klabunde, H. F. Efner, L. Satek, and W. Donley, *J. Organomet. Chem.*, **71**, 309 (1974).
- (2) The solvents do not react with the metal atoms at the very low temperatures employed although weak σ - and/or π -coordination is important.
- (3) K. J. Klabunde, H. F. Efner, and T. O. Murdock, Seventh International Conference on Organometallic Chemistry, Venice, Italy, Sept 1975.

- (4) R. Niedermayer, *Angew. Chem.*, **87**, 233 (1975); *Angew. Chem., Int. Ed. Engl.*, **14**, 212 (1975).
- (5) L. A. Hanlen and G. A. Ozin, *J. Am. Chem. Soc.*, **96**, 6324 (1974).
- (6) For review of metal atom-organic chemistry, see K. J. Klabunde, *Acc. Chem. Res.*, **8**, 393 (1975).
- (7) K. J. Klabunde and H. F. Efner, *J. Fluorine Chem.*, **4**, 116 (1974).
- (8) P. S. Skell, Symposium on "Atomic Species Used in Synthesis", INOR, paper 57, 170th National Meeting of the American Chemical Society, Chicago, ILL., Aug 1975.
- (9) J. H. Sinfelt, *J. Catal.*, **29**, 308 (1973); *Catal. Rev.*, **9**, 147 (1974).

K. J. Klabunde,* H. F. Efner
T. O. Murdock, R. Ropple

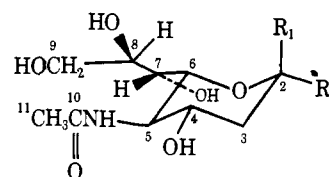
*Department of Chemistry, University of North Dakota
Grand Forks, North Dakota 58202
Received September 29, 1975*

¹³C Spin Lattice Relaxation in the Neuraminic Acids. Evidence for an Unusual Intramolecular Hydrogen Bonding Network¹

Sir:

N-Acetylneuraminic acid (NANA) and its derivatives play an important role in the chemical and physical interactions of the glycoproteins and glycolipids associated with biomembranes, where it is bound ketosidically in the α anomeric form.² Therefore, we have decided to explore in some detail the structures and conformations of the neuraminic acids. Several recent reports have shown the utility of ¹H NMR and ¹³C NMR in the study of NANA and NANA containing molecules.³ We wish to report the first ¹³C spin lattice relaxation (T_1) study of NANA and its derivatives and to demonstrate the potential of this parameter to provide unique insight into the structural understanding of these important biomolecules.

NANA (**1a**) was prepared from edible birds nest substance using a modification of existing published procedures.⁴ Methyl β -D-*N*-acetylneuraminidate (**1b**) and 2-*O*-



- 1a**, $R_1 = \text{OH}$; $R_2 = -\text{CO}_2\text{H}$
1b, $R_1 = \text{OH}$; $R_2 = -\text{CO}_2\text{CH}_3$
1c, $R_1 = \text{OCH}_3$; $R_2 = -\text{CO}_2\text{H}$
1d, $R_1 = -\text{CO}_2\text{H}$; $R_2 = \text{OCH}_3$

methyl- β -D-*N*-acetylneuraminic acid (**1c**) were prepared by the method of Kuhn et al.⁵ The modified Koenigs-Knorr synthesis of Meindl and Tuppy was used to prepare 2-*O*-methyl- α -D-*N*-acetylneuraminic acid (**1d**).⁶ Free acids were converted to their sodium salts by titration with NaOH solution followed by lyophilization. In order to minimize the effects of paramagnetic impurities, that seem especially prevalent in D_2O solutions, the sample preparation techniques suggested by Roberts and co-workers⁷ were used.

We have examined the ¹³C NMR of the four neuraminic acid derivatives. The $T_{1\text{obsd}}$ values and corresponding nuclear Overhauser enhancements (η) are presented in Table I. Chemical shift values and assignments, which correspond closely to previously published data,^{3a,b} have been omitted due to space limitations. All values represent the mean of three-five individual determinations, for which the standard deviations were ± 10 –15%. The values for $T_{1\text{DD}}$, which represent the contribution to the total relaxation from the direct dipole-dipole mechanism, were calculated from the